
Article:

Califano, M orcid.org/0000-0003-3199-3896, Skibinsky-Gitlin, ES, Gómez-Campos, FM et al. (1 more author) (2019) New strategies for colloidal-quantum-dot-based intermediate-band solar cells. The Journal of Chemical Physics, 151 (15). 154101. ISSN 0021-9606

https://doi.org/10.1063/1.5121360

New Strategies for Colloidal-Quantum-Dot-Based Intermediate-Band Solar Cells

Marco Califano,*,† Erik S. Skibinsky-Gitlin,‡ Francisco M. Gómez-Campos,‡,¶
and Salvador Rodríguez-Bolívar‡,¶

Pollard Institute, School of Electronic & Electrical Engineering, and Bragg Centre for Materials Research, University of Leeds, Leeds LS2 9JT, United Kingdom, Departamento de Electrónica y Tecnología de Computadores, Facultad de Ciencias, Universidad de Granada, 18071 Granada, Spain , and CITIC-UGR, C/ Periodista Rafael Gómez Montero, n 2, Granada, Spain

E-mail: *m.califano@leeds.ac.uk

Abstract

The intermediate-band solar cell (IBSC) concept promises to increase the efficiency limit in a single-junction solar cell through the absorption of below-bandgap-energy photons. Despite their operating principle having been proposed over 20 years ago, IBSCs have not delivered on this promise yet, and the devices fabricated so far, mainly based on embedded epitaxial quantum dots, have, instead, operated with lower efficiency than conventional solar cells. A new paradigm, based on the exploitation, as intermediate band, of the intra-gap states, naturally occurring in the density functional theory description of *colloidal* (i.e., chemically synthesized) quantum dots, was

---

*To whom correspondence should be addressed

†Pollard Institute, School of Electronic & Electrical Engineering, and Bragg Centre for Materials Research, University of Leeds, Leeds LS2 9JT, United Kingdom

‡Departamento de Electrónica y Tecnología de Computadores, Facultad de Ciencias, Universidad de Granada, 18071 Granada, Spain

¶CITIC-UGR

suggested recently. Here we revisit this intriguing concept unveiling its shortcomings and propose two alternative schemes: in the first, the localised electron surface trap states, ubiquitously found in commonly synthesized colloidal quantum dots, are used as intermediate bands in strongly coupled films made of small InAs nanocrystals; in the second scheme, the intermediate band is provided by the conduction-band-minimum-derived miniband in films of larger InAs nanocrystals. Both schemes yield estimated limiting IBSC efficiencies exceeding Shockley-Queisser's limit for a single absorber.

Keywords: *Optical transitions, nanocrystal films, colloidal quantum dot superlattices, pseudopotential method*

INTRODUCTION

Conventional solar cells made of a single absorber can harvest only photons with energy equal or higher than the band gap of the active material, resulting in a wasteful loss of about 25% of the solar spectrum, represented by lower-energy photons (typically those with energy smaller than 1.0-1.5 eV). Furthermore, the photon energy in excess of the band gap is lost to lattice vibrations, i.e., heating of the cell, which is also detrimental to the device's performance. A possible strategy to overcome the former limitation and to increase by over 50% (from 31% to 46.8% at 1 sun, and from 40.7% to 63.2% at full concentration) the efficiency limit in a single junction solar cell exploits the Intermediate-Band Solar Cell (IBSC) concept,[1–4] where the creation of a partially occupied intermediate band (IB) in the gap between the valence band (VB) and the conduction band (CB) of the active material allows the absorption of sub-bandgap photons. The latter can use the IB as a sort of "stepping stone", to promote electrons from the VB to the CB in a two-step process: VB→IB from the VB into the empty states of the IB, and IB→CB from the occupied states of the IB into the empty states of the CB, in addition to the traditional

VB→CB band gap absorption. This strategy has the added advantage of simplicity, as it dispenses from the need to introduce additional material layers, as in the case of a tandem cell, avoiding complications in the growth process.

Although a few schemes to build bulk IBSCs have been proposed and realised,[2] the main implementation of the IBSC concept has been based so far on epitaxial quantum dots (EQDs - mainly made of InAs) creating the intermediate band when they are embedded in a wide gap barrier material (GaAsX).[2] Unfortunately nearly all of the devices fabricated using these materials performed poorly and even their very operation as actual IBSCs was questioned.[2] Furthermore, all EQD IBSCs manufactured so far exhibited a loss of voltage (from room temperature to very low temperatures) with respect to control cells without QDs.[4] The reasons for that are not completely understood and still debated. One of the problems is that the system used - InAs EQDs in a GaAs matrix - although well characterised experimentally and considered as a "standard" in quantum dot physics, being based on a well-established and mature technology, is indeed far from realising the ideal conditions needed for IBSC operation,[3] with the IB-CB gap of the order of 100-200 meV at most.[5] Furthermore, measured efficiencies have never exceeded those obtained for the control cell without QDs. A conclusive proof that a device is operating as an IBSC would be the detection in its emission of three different wavelengths,[6] corresponding to the three possible transitions (VB to IB, IB to CB and VB to CB). Unfortunately this three colour emission has been reported only in GaN_xAs_{1-x} based IBSCs.[7]

Recently an intriguing scheme was proposed,[8] where the intra-gap states (IGSs) naturally occurring in the density functional theory (DFT) description of colloidal quantum dots (CQDs) following structural relaxation,[8] were suggested as viable intermediate bands for implementing the IBSC concept in arrays of CdSe nanocrystals (NCs).

Although that work seemed to present a compelling case for IGSs as IBs, its conclusions were based on DFT calculations on small clusters ($Cd_{15}Se_{15}$ with $R \sim 0.6$ nm). This is of particular relevance considering that the band gap of dots of that size (which were used as building blocks for the arrays exhibiting IB formation in Ref. 8), although of the order of 1.5-2.0 eV according to the results of DFT modelling,[8] exceeds 3.6 eV[11] when measured in real systems. Indeed, the material considered in Ref. 8 (CdSe) is not ideal for such IBSC applications, given its large band gap (1.7 eV) in the bulk. Therefore, for a realistic implementation of the IBSC concept, larger NCs made of small band gap materials should be considered as building blocks. As the electronic, structural, and chemical properties of very small nanoparticles with a few tens of atoms have been shown both theoretically and experimentally[9] to be more sensitive on surface interactions than their larger (and more commonly experimentally synthesised) counterparts, the question that needs to be addressed is whether the results of Ref. 8 can be generalised to dots with radii in the experimental range ($R > 1.0$ nm) and with a total number of atoms exceeding 160. Indeed, we have shown recently[10] that the band structure of NC films is very material- and size-sensitive: films made of small dots can exhibit very different features from those made of large NCs, due to the much reduced coupling experienced by the dots with increasing size. Also, we found[10] the width of the CBM-derived miniband, that forms when the dots are brought close together in CdSe NC films, to be nearly 6 times smaller (67 meV vs 392 meV) than that calculated for films of InAs of the same size ($R = 1.2$ nm). Finally, the IGSs considered in Ref. 8 were completely delocalised. Considering that, in general, the deeper a gap state, the smaller the hydrogenic radius of its wave function (i.e., the stronger its localisation),[12] the 0.4 to 0.6 eV depth of the IGS states calculated in Ref. 8 would seem to preclude a large delocalisation. Instead, their degree of delocalisation was so high (higher, in fact, than most of the VB states and some of the CB states, including the CBM, in the same dot), that it is questionable whether their identification as IGSs, rather than as proper band edge states, is justified. Interestingly, no IGS were identified by previous time-domain DFT calculations on the same systems.[13] We therefore conclude that the IGSs considered in Ref. 8 are not representative of the most common type of IGSs observed in semiconductor nanocrystals of experimentally relevant sizes: surface traps.

Here we revisit the concept of using IGSs as IBs in CQD films, aiming to test its applicability to realistically sized nanocrystals made of a more suitable material - InAs (bulk band gap 0.4 eV) - for the implementation of the IBSCs concept. This investigation will be carried out within the framework of the state-of-the-art atomistic semiempirical pseudopotential method (see Supporting Information for further details), that has proved successful in the past in accurately determining band edge positions,[11] absorption[14] and transport[15] properties of semiconductor nanocrystals of different materials, as well as in modelling both hole[16] and electron[17] trap states and their population dynamics.[18]

RESULTS

The IGS we consider is an electron surface trap (see Fig. S1, Supporting Information), whose ubiquitous presence in nanocrystals of many different materials has been extensively documented experimentally.[9,19–21] We first investigate its suitability as an IB in small nanocrystals (starting with the same size as the one considered in Ref. 8, $R = 0.6$ nm, up to $R = 1$ nm, containing from 29 to 147 atoms), by verifying that it satisfies the following necessary minimum conditions: (i) the IGS is separated by a zero density of states from both VB and CB; and (ii) the VB→IGS and IGS→CB transitions are optically allowed and strong. An energetically isolated IGS [condition (i)] is required in order to maintain three well-separated quasi-Fermi levels, which are essential to preserve the high output voltage of the cell.[2,5] This condition will also contribute to suppress non-radiative recombination, if the VB-IGS and IGS-CB separations are much greater than the LO phonon energy. The necessity of condition (ii) is evident. We note that the additional condition of a finite width for the IGS-derived miniband[8] to guarantee the presence of both empty and occupied states to support both (VB→IB) transitions into it and (IB→CB transitions) out of it,[1,2] is not necessary as, statistically, in a large ensemble some IB states will be occupied while others will be empty, providing the required half-filling. This condition is not even required for transport, as in an IBSC the carriers should be collected from CBM and VBM, but not from the IB, in order to maintain a large V_{oc}.[1,2] A large IB width, on the other hand, can even be detrimental to the conversion efficiency, as we will show later on in this work, as it can lead to voltage drops that are proportional to it.

The calculated optical spectra for the isolated dots (representing the dilute solution case), show that the IGSs of all three sizes (Fig. S2, Supporting Information) satisfy conditions (i) and (ii). However, it is clear that the oscillator strength of the transitions involving the IGS (IGS→CB and VB→IGS) decreases with increasing dot size, becoming about one order of magnitude smaller than the band edge transition VBM→CBM for $R = 1$ nm, consistently with the room temperature experimental signature of these trap states being observed as a low intensity broad shoulder to the low energy side of the main optical gap,[9,19,20] in nanocrystals of experimental size. Nevertheless, the three-colour photon emission, critical proof of the correct behaviour of the IB,[6] should be clearly detectable in all three nanostructures. It is clear, however, that, even though InAs has a bulk band gap of 0.4 eV, compared to 1.7 eV for CdSe, the energy of the VBM→CBM absorption edge of a dot with $R = 0.6$ nm is too high (> 3 eV) for optimal solar conversion efficiency in an IBSC (although, in principle, this value of the band gap could still lead[22] to efficiencies in excess of the Shockley-Queisser limit,[24] the position of the IB in this case leads to much lower efficiencies, see Table 1), for attaining which a band gap around 2 eV represents the ideal case.[22]

Based on the energies of the different transitions for the isolated dots, we estimated, according to Bremner, Levy and Honsberg,[23] and Krishna et Krich,[22] IBSCs limiting efficiencies exceeding the Shockley-Queisser (SQ) limit[24] (and the estimated performance of small CdSe clusters[8]) for the two larger dots (see Table 1) both at 1 and 100 suns.[22,23]

The calculated band structure of arrays made of these dots shows (Figure 1) a remarkable IB width of about 400 meV, in the smallest dot, that decreases to 20 meV for $R = 0.8$ nm, and becomes completely flat in the largest dot ($R = 1.0$ nm), even for the closest

Table 1: IBSC limiting efficiencies at 1 sun (AM1.5G) and 100 suns (AM1.5D), estimated according to Bremner, Levy and Honsberg[23] and to Krishna and Krich,[22] for InAs NCs both isolated and in a close-packed film. (The transition energies used in the estimate are reported in Table S1, Supporting Information). For comparison, the SQ limit for nanostructured solar cells is 32.7% at 1 sun and 36.6% at 100 suns.[34] For $R \leq 1.0$ nm the IB is the IGS, whereas in the case of $R = 1.2$ nm and $R = 2.0$ nm the CBM is considered as the IB.

	Isolated		Film	
R[nm]	η(1 sun)[%]	η(100 suns)[%]	η(1 sun)[%]	η(100 suns)[%]
	IB=IGS			
0.6	< 30	~ 30	$\lesssim 30$	~ 35
0.8	~ 37	39-44	40-43	52-54
1.0	~ 46	52-54	43-45	48-52
	IB=CBM			
1.2	~ 38	45-50	48-49	54-55
2.0	~ 43	52-54	40-43	48-52

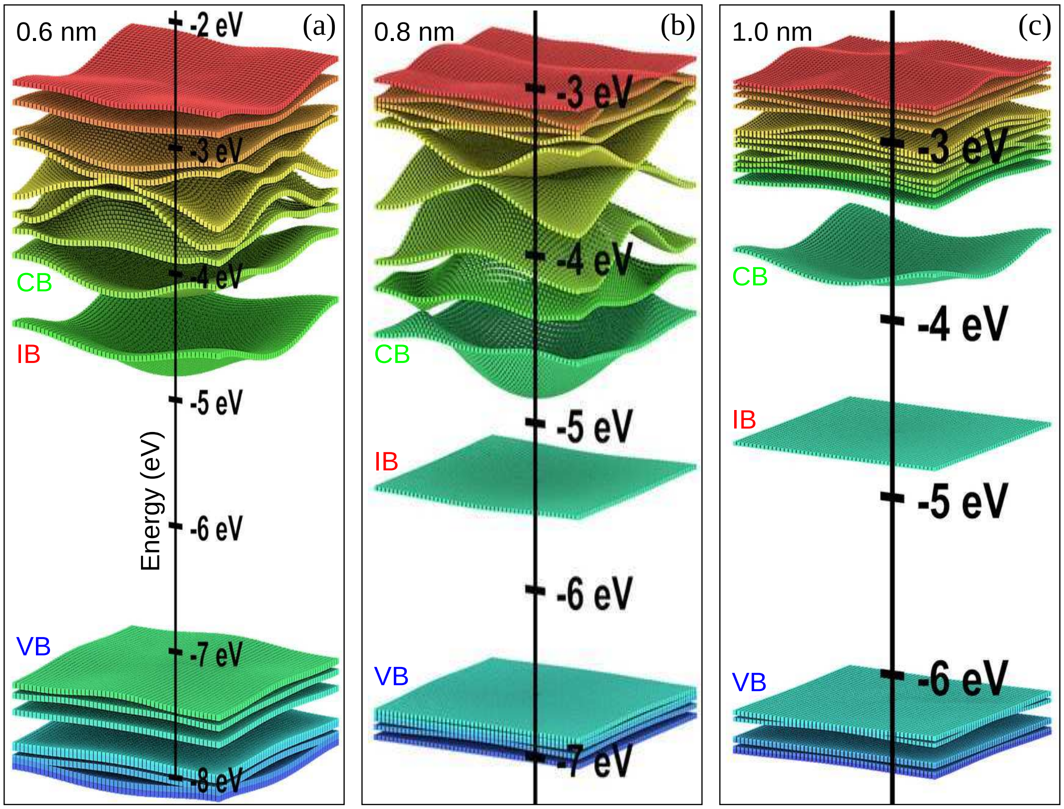

Figure 1: Band structures of films of InAs CQDs with $R = 0.6$ (a), 0.8 (b), and 1.0 nm (c). The energies are referred to the vacuum level.

interdot separation realistically achievable (1 bond length).

This is due to the localised character of the surface trap states we consider as IGS, so that the probability that their wave function will overlap with that of a neighbouring dot in the array becomes increasingly small the larger the radius, no matter how close the dots may be.

Figure 1 further suggests that the band structure of arrays made of very small clusters may be very different from that of films made of nanocrystals with experimentally relevant sizes. Indeed we recently found[10] that the width of the miniband associated with the CBM decreases according to a $\approx D^{-2}$ (where $D = 2R$) dependence, in films of CdSe NCs. The size effect was even more dramatic in InAs, where an increase by less than a factor of 2, from 1.2 nm to 2 nm, in the radius of the array's building blocks, led to a decrease by a factor of 8, from ~ 400 meV to 50 meV, in the CBM miniband width. Here we also find a significant downward shift of the CBM miniband in films of NCs with $R = 0.6$ nm and 0.8 nm, compared to the position of the CBM in isolated dots of the same size (this shift is clearer from the 2D band structure displayed in the right-hand panels of Figure 2). Such shift is independent of the presence of either the IGS or the VB states, but is due to the coupling of the CBM with higher CB states in neighbouring NCs (see Fig. S4, Supporting Information).

Interestingly, we find that the IB→CB transition can be either red- or blue-shifted compared to the IGS→CB transition in isolated dots (red dashed lines in Figure 2), depending on the specific band structure characteristics. We should also mention that our calculations were performed for the ideal IBSC operating conditions of half filling of the IB, i.e., with the quasi-Fermi level relative to the IB positioned in the middle of that band. This configuration can be achieved through photodoping (although this procedure is better suited for high solar concentrations[35]) or electronic doping (as discussed in Ref. 8). For wide IBs, as in the case of the smallest dot, half-filling means that the onset of the IB→CB transition is determined by the IB-CBM separation away from the Γ point and closer to

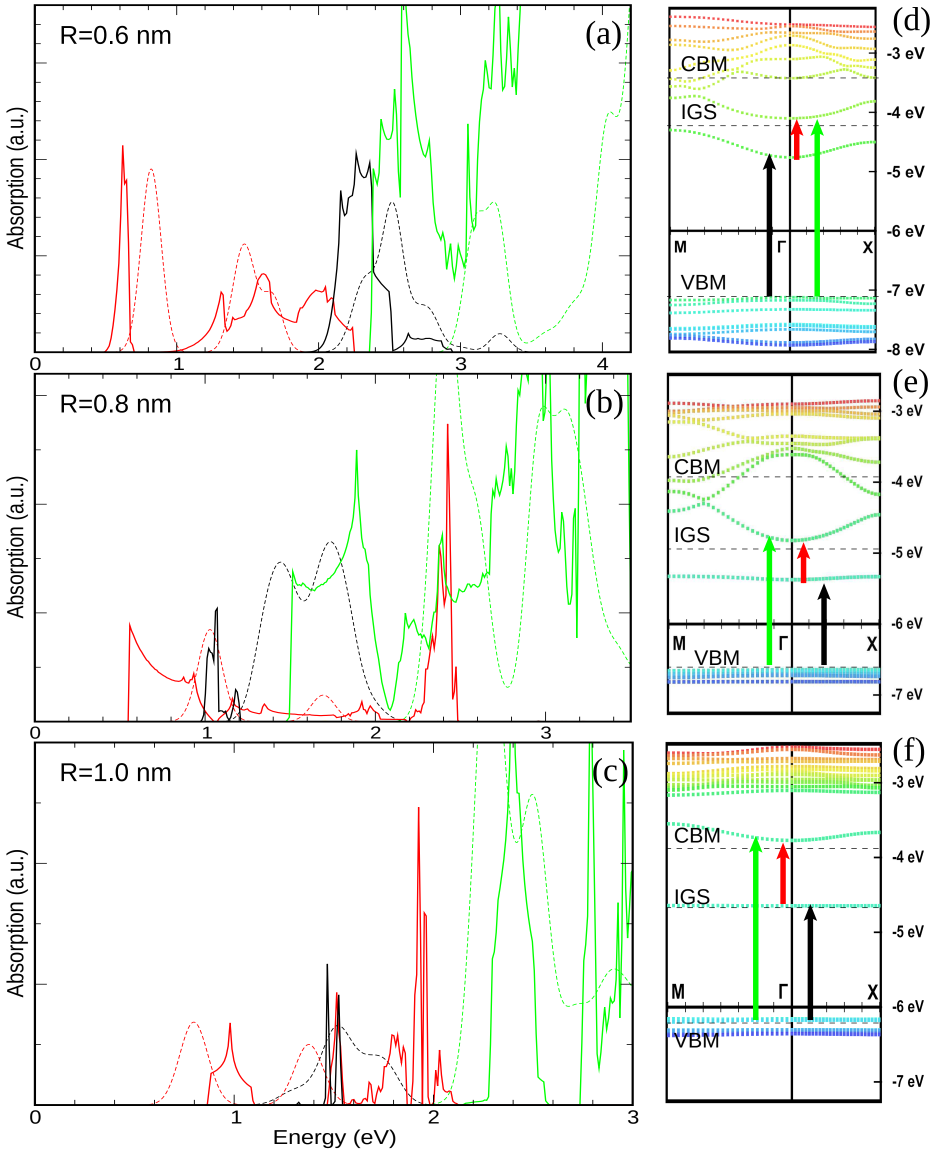

Figure 2: (a)-(c) Absorption spectra of films (solid lines) and isolated (dashed lines) InAs CQDs with $R = 0.6$ (a), 0.8 (b), and 1.0 nm (c). For clarity, the spectra of the films have been rescaled so that the amplitude of the main IB→CB transition peak (red lines) was the same as that relative to isolated dots. (d)-(f) The calculated band structure (Figure 1) is shown in a 2D representation (right-hand panels) to aid in the identification of the different transitions (coloured arrows). The absorption curves are colour-coded with the arrows in the band structure (and the inset of Fig. S2, Supporting Information).

the Brillouin zone boundary. The large red shift exhibited by the NC with $R = 0.8$ nm is instead due to the large coupling between CBM and higher CB states that, leading to a widening of the CBM miniband, brings it closer to the IB, even despite the latter's shift to lower energies compared to the position of the IGS in the isolated dot (black horizontal dashed lines in Figure 2). The blue-shifted IB→CB transition found in the case of the largest NC originates from the upward shift of the CBM, that compensates for its widening.

The onset of the other two transitions (VB→IB - black lines in Figure 2 - and VB→CB - green lines in Figure 2) is instead either red-shifted ($R = 0.6$ nm and 0.8 nm) or not shifted at all ($R = 1.0$ nm), as the VBM is flat (so its position corresponds to that in the isolated dot), and any width in either CBM or IB translates into a downward bowing that brings them closer to the VB. The red shifts in the $R = 0.8$ nm dot have instead a completely different origin: although the IB is quite flat and its width would only cause negligible red shifts, it exhibits, however, a large rigid shift downwards, compared to the position of the IGS, due to an unusually large negative value for the overlap integral

$$\left\langle \psi_{IGS}(\vec{r}) \middle| V(\vec{r} - \vec{R}_p) \middle| \psi_{IGS}(\vec{r}) \right\rangle$$

(where $\vec{R}_p$ is the position of a neighbouring NC in the array), contributing to the miniband's energetic position (but not to its width) in the tight-binding approach[36] used to solve the Schrödinger equation of the NC film. We conclude that the optical properties of closely packed NC films are quite different from those of diluted solutions, and cannot be simply deduced from the study of isolated dots.

Based on the position of the absorption peaks for the different transitions, we again estimate[22,23] IBSCs limiting efficiencies exceeding the SQ limit[24] for the two larger dots (see Table 1) both at 1 sun and at 100 suns.[22,23]

We note that the above results were obtained for ideal 2D arrays (see Supporting Information for the details of our model). The performance of realistic NC-film-based IBSC devices may be affected by the presence of disorder (either due to the polydispersity of the dots' sizes, or to fluctuations of their positions) in the film, which, by breaking the system's periodicity, would alter the array's wave functions. We expect this effect to have a larger impact on the film's mobility[10,15] than on its optical properties, where it may introduce some additional broadening of the spectra and variations in their amplitude, both of which may lead to a voltage reduction. However, while a broad excitonic peak, by enabling light absorption across a wider spectral range, also leads to high current densities, the presence of tail states below it only leads to a reduction in the voltage of the cell.[52]

Taking advantage of the large energy separation in CQDs between the s-like CBM and the p-like excited states, which in our systems can easily be made to exceed 500 meV in isolated dots, and of the large width of the minibands derived from both sets of states in a dot array[10] (these minibands will henceforth be denoted as M_n, with $n = 1$ for the CBM-derived miniband and $n = 2, 3, 4$ for minibands originating from the triplet of p-like states), we will now explore an alternative scheme for the implementation of IBSCs: the use of M_1 as a potential IB candidate. This choice is not unreasonable, considering that M_1 automatically satisfies both minimum IB suitability conditions mentioned above, and that, moreover, it allows harnessing of the energy in excess of the nanocrystal's bandgap through the "extended" bandgap transition VB$\rightarrow M_{2,3,4}$. Indeed, the "standard" VB→IB, VB→CB, and IB→CB transitions become the VB$\rightarrow M_1$, VB$\rightarrow M_{2,3,4}$, and $M_1 \rightarrow M_{2,3,4}$ transitions in our scheme. In this case, in order to engineer the "band gap" VB$\rightarrow M_{2,3,4}$ transition to ideal values for IBSC implementation (1.9-2.4 eV), we consider dots with $R = 1.2$ nm and 2.0 nm.

We find that: (I) the absorption spectra of isolated dots of both sizes (Fig. S3, Supporting Information) exhibit the required characteristics for their implementation in IBSCs, (based on the energies of the different transitions, reported in Table S1 Supporting Infor-

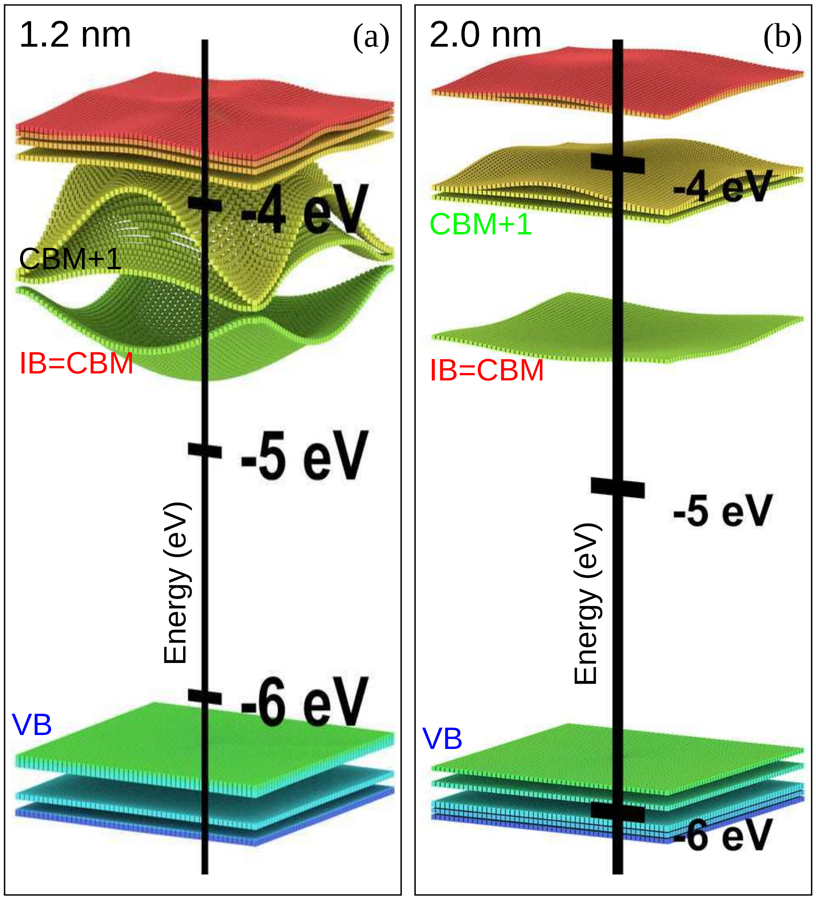

Figure 3: Band structures of films of InAs CQDs with $R = 1.2$ (a) and 2.0 nm (b). The energies are referred to the vacuum level.

mation, we estimated[22,23] limiting efficiencies exceeding SQ's limit at both 1 sun and 100 suns - see Table 1); (II) when they are assembled in close packed arrays (films), the width of all relevant M_n minibands exceeds 50 meV (Figure 3); finally, (III) the films' absorption spectra (Figure 4) also maintain the desirable characteristics exhibited by isolated dots, showing, however, in the case of $R = 1.2$ nm, a blue shift in the $M_1 \rightarrow M_{2,3,4}$ transition (red solid line in Figure 4), and a red shift in the VB→M_1 transition (black solid line in Figure 4), compared to single nanocrystals (all transitions involving the VB include the effect of Coulomb attraction between electron and hole). The latter effect is consistent with what is observed experimentally in many different materials[37–41] in going from dilute solutions to close-packed solids.

Although the two shifts have opposite directions, both have the same origin: the strong coupling occurring when the dots are brought close together in an array. This effect, that, due to the lighter electron effective mass is stronger in the CB than in the VB (as confirmed experimentally for PbSe and InAs CQD films[38,39]), is responsible for the formation of minibands which are wider, the stronger the coupling (i.e., the closer the dots), and ultimately leads to band-like transport and high electron mobility in these systems.[41,42] Since (A) the miniband widening occurs through the lowering of the minibands' minimum energy (which is located at the Γ point for VBM and M_1, and at the Brillouin zone boundaries for $M_{2,3,4}$ - Figure 3), and (B) the transitions with the largest oscillator strength originate from regions close to Γ (Fig. S5, Supporting Information), the net result is a larger *optical* separation between M_1 and $M_{2,3,4}$ on one hand (as the minimum *energetic* separation between them is actually much reduced, as clearly visible from Figure 3, a low energy tail appears in the absorption peak), and a reduced *optical* separation between the VBM and M_1, on the other. This is a further indication that single-dot calculations cannot predict the absorption features of a densely packed film. Both shifts decrease with increasing interdot distance, until they converge, respectively, to the $e_1 - e_2$ energy level separation and the band gap absorption edge of the isolated dots, for suf-

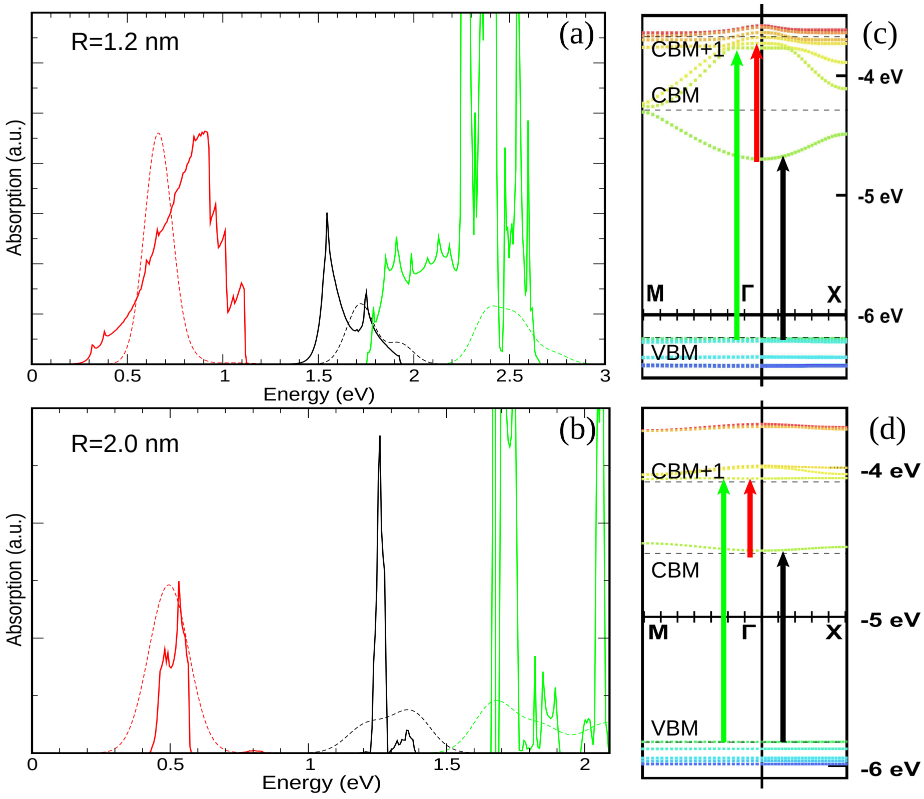

Figure 4: (a)-(b) Absorption spectra of films (solid lines) and isolated (dashed lines) InAs CQDs with $R = 1.2$ (a), and 2.0 nm (b). For clarity, the spectra of the films have been rescaled so that the amplitude of the main IB→CB transition peak (red lines) was the same as that relative to isolated dots. (c)-(d) The calculated band structure (Figure 3) is shown in a 2D representation (right-hand panels) to aid in the identification of the different transitions (coloured arrows). The absorption curves are colour-coded with the arrows in the band structure.

ficiently large distances (Fig. S6, Supporting Information). Even with the new, shifted, IB-CB and VB-CB gaps, the estimated limiting efficiencies of IBSCs made with the two structures still exceed SQ's limit at both 1 sun and 100 suns (Table 1).

We want to stress here that these are ideal upper efficiency limits, obtained, within the detailed balance framework, assuming (a) the carrier mobilities to be infinite, (b) the only recombination process to be radiative, and (c) complete absorption of all photons with energies above the threshold for the lowest transitions. These clearly idealised conditions are useful to estimate upper limits, and to provide a common standard for comparing the performance of different devices, but - especially in the case of (a) and (b) - can only be considered as approximations to real systems. The performance of actual IBSC devices made using InAs nanocrystals as building blocks may therefore differ quite strongly from the values reported in Table 1.

We recently estimated upper bounds for the electron mobility (a) in films of InAs NCs with $R = 1.2$ nm and 2.0 nm to be of the order of 2.6 and 0.4 cm^{2}V^{-1}s^{-1}, respectively,[10] whereas the radiative lifetime in the largest (isolated) dot was calculated[25] to be 0.54 μs. Assuming the mobility to be proportional to the miniband width (for dots of the same material), we expect it to be of the same order of magnitude in the three dots with smaller sizes considered above. A recent study[26] found the recombination rates (b) in PbS-NCs-based solar cells to be mobility-dependent and controlled by diffusion of free charge carriers to trap states. The measured free carrier mobility increased with decreasing dot size, in agreement with our findings. This increase led, on one hand, to a decrease in the open circuit voltage (V_{oc}), as the charge carriers could find more quickly recombination centres (whose density was found to increase with decreasing size), and on the other to improved charge extraction, hence to a larger short circuit current J_{sc}. They concluded that, owing to this delicate balance between J_{sc} and V_{oc}, NC films with mobilities in the range 10^{-3} to 10^{-2} cm^{2}V^{-1}s^{-1} should result in solar cells with better power conversion efficiencies than films with larger values for the mobility. Based on this analysis, IBSCs using our largest NCs should achieve the best conversion efficiency.

Finally, regarding assumption (c), the discrete nature of the conduction band electronic structure in isolated dots, where the separation between CBM and CBM+1 is of the order of a few hundreds of meV, generally gives rise to an absorptionless window of a similar width at energies above the IB→CBM transition (The gaps above the VB→IB transitions, visible in Figure 2 and Figure 4, originate, instead, from the limited number of valence band states included in the calculations, whose main focus was the determination of the transition's absorption edge. Such gaps are expected to vanish following the inclusion of a sufficiently large number of VB states). As these gaps in the conduction band of isolated dots decrease with increasing size, films of larger NCs may seem a more suitable choice for IBSCs exploiting scheme I. However, despite the larger gap in their electronic structure at the single-dot level, films of $R = 0.8$ NCs outperform those made of $R = 1.0$ NCs from this point of view and exhibit an uninterrupted absorption spectrum (compare panels b and c in Figure 2). This is due to their peculiar miniband structure with wide CB-derived minibands and a flat IB, which lead to a red shift in the IB→CBM transition energy threshold (at Γ), and, owing to the opposite curvature of CBM and CBM+1, to the filling of the gap between these minibands, due to the presence (for $\vec{q} \neq 0$) of an almost continuous spectrum of energies between the minimum of the CBM and the maximum of the CBM+1 minibands.

Another indication that larger NCs may be better suited as building blocks for IBSCs comes from the observation that the molar extinction coefficient in NCs increases with size,[14,27–33] leading to a stronger absorption in films made of large dots, for the same nominal film thickness (i.e., for the same number of dot layers. Equivalently, a given absorption can be obtained with thinner films if made of large dots).

The critical role played by the film's band structure, combined with the (often contrasting) size-dependent features of the isolated dot electronic structure (such as the gaps between different states), and optical properties (such as the extinction coefficient) make it difficult to identify an ideal size (or size range) for application in scheme I IBSCs. However, given their high estimated limiting conversion efficiencies (Table 1), together with their continuous absorption spectrum, films of $R = 0.8$ NCs represent our choice as an ideal size to implement scheme I.

That larger NCs may indeed be better suited as building blocks for IBSCs for the second scheme we proposed is instead suggested (together with the arguments discussed above), by the observation that the peculiar band structure of films of dots with $R = 1.2$ nm (Figure 3 and Figure 4, upper right-hand panel), may lead to a reduction in the IBSC efficiency, if following an optical ~ 0.9 eV IB→CB (i.e., $M_1 \rightarrow M_{2,3,4}$) transition at Γ, the electron thermalized rapidly to the Brillouin zone edges, leading to a significant (~ 0.5 eV) voltage loss. Moreover, the small energetic separation between M_1 and M_2 at this position in k-space could favour a further phonon-assisted relaxation back to the IB (M_1), causing a current loss. Even from this point of view, dots with $R = 2.0$ nm represent a better alternative, as, due to the large and nearly constant energetic separation between M_1 and $M_{2,3,4}$ in k-space (Figure 3 and Figure 4, lower right-hand panel), they are not susceptible to any of these loss mechanisms. If increasingly larger sizes would have the additional advantage of a narrower separation between higher CB minibands (leading to a reduce absorptionless window above the IB→CBM transition onset, as discussed above), they would also exhibit a narrower band gap, leading, for $R > 3.5$ nm, to a drop of the associated limiting conversion efficiency, in our second IBSCs scheme (where the effective band gap is given by $E_g = E(CBM+1) - E(VBM)$), below the SQ limit.[22,23] We therefore conclude that NCs with $2 < R < 3.5$ nm are the most suitable for implementation of scheme II.

It is also worth mentioning that these results were obtained, as in the case of smaller NCs, at room temperature (300 K) and with the quasi-Fermi level relative to the IB (M_1, in our case), positioned in its middle, so that the IB is half filled in order to provide both empty states for the VB→IB transitions, and occupied states for the IB→CB transitions.[1]

The main effect on the absorption spectra of this upwards shift in the Fermi level, from the position in the VB-CB gap (i.e., below M_1) it would have in undoped structures, is to reduce the blue shift in the IB→CB (i.e., $M_1 \rightarrow M_{2,3,4}$) transition, by introducing a low-energy shoulder in the absorption spectra, as M_1 electrons at Γ are now half a miniband width higher in energy than before. Also contributing to this shoulder are the many direct transitions from M_1 to $M_{2,3,4}$, originating from the remaining regions of the newly populated Brillouin zone.

Before we conclude, we will briefly discuss the main challenges facing QD-based IBSCs: (1) charge extraction, (2) optimal carrier occupancy in the IB, (3) excitonic nature of the absorption spectrum. (1) In order to maintain a high V_{oc}, carriers should only be collected from the CBM and the VBM, but not the IB.[1,2] Achieving this in NCs may be challenging, considering that colloidal dots are not embedded in a matrix (like epitaxial dots), and therefore they (and hence all three bands) are in direct contact with the electrodes. Possible strategies to isolate the IB include the use of a charge-selective extraction layer in the proximity of the electrodes or of an IB blocking layer near the electron-collecting electrode.[7] The identification of specific extraction layers suitably matched to CBM and VBM for electron and hole collection is, however, beyond the scope of the present investigation. Recent work on PbS-nanocrystal-based solar cells[26] indicated ITO and LiF/Al/Ag as suitable electrodes, whereas TiO_2 was suggested for electron extraction in CdSe-based devices.[43]

The challenges in charge collection are partially mitigated by the consideration that the IBSC features a "natural" connection between its two "sub-cells", compared with that obtained, often with significant processing effort, in a monolithic 3-cell tandem structure[53] with which it shares the calculated limiting efficiency.

(2) As we mentioned above, the IB must be half filled in order to provide both empty states for the VB→IB transitions, and occupied states for the IB→CB transitions.[1] Conventional (i.e., epitaxial) QD-based solar cells suffer from low occupancy of the IB, which

leads to a strong bleaching of the IB→CB transition, hence to current losses.[44] This problem is being addressed by (i) trying to fabricate high-density arrays of small and homogeneous dots with low defect and long radiative lifetimes[45] (achieving these conditions has proven extremely challenging due to the build-up of high internal strain in the growth process,[46] which not only results in an increase in the dot size and its fluctuations, but also negatively affects solar cell performance[47]), and (ii) doping (either through electrical[48] or optical[49] routes). The use of colloidal QDs represents a huge advantage over epitaxial dots from this point of view as, owing to their chemical nature, they can be synthesized with very accurate size control and monodispersity and easily assembled in high-density, virtually defect-free, 3D superstructures, and their surface can be effectively passivated (either by using organic/inorganic ligands or by doping) to remove all trap states.[41,42,50,51]

(3) The discreteness of the electronic states and the ensuing discrete character of the excitonic optical transitions in NCs may significantly reduce the single junction conversion efficiency, by reducing the photogenerated current.[52] The main origin of this effect is the transparency of the NC absorption spectrum between sets of absorption peaks, which is more pronounced for $R = 0.8$ nm and 2.0 nm, but is also present in all other sizes (see Figure 2 and Figure 4). However, CQDs-based IBSCs have two additional advantages: minibands with a finite width and absorption rates that increase with increasing energy. Both properties are crucial to achieve conversion efficiencies beyond the SQ limit as they ensure the participation of photons of the lowest possible energy in the available absorption processes, avoiding the loss of photon energy in excess of the energy gap.[53] When high and low energy absorption processes compete, the required photon selectivity is "naturally" achieved in CQD-based IBSCs, where higher energy processes are more strongly absorbing compared to lower ones as apparent from Figure 2 and Figure 4. The finite miniband width introduces, however, an upper bound on the energy of the absorbed photons, which, in practice is not likely to lead to significant losses, considering

that such photons are already filtered by the atmosphere or by the use of ultraviolet absorbers (protecting the cell encapsulation), providing a similar high energy cut-off.[53]

CONCLUSIONS

In conclusion, we have revisited a promising IBSC scheme, based on the use of electronically isolated states in CQDs films as IBs. We have shown the unsuitability of the original proposal and suggested two alternative schemes: in the first, the localised electron surface trap states (as opposed to the very delocalised DFT-derived IGS proposed in Ref. 8), ubiquitous in commonly synthesised CQDs, are used as IBs in NC films made of a suitable (i.e., small band gap) material, InAs (as opposed to wide-band-gap CdSe used in Ref. 8). We found that in films made of very small dots these states yield very wide IBs which may lead to large voltage drops, furthermore the energies of the resulting optical transitions are too large for IBSCs based on these nanostructures to yield solar conversion efficiencies in excess of (or even close to) SQ's limit for a single absorber. Although larger NCs exhibit very narrow IBs, show strong IB→CB transitions and, based on the position of their absorption features, have the potential to exceed SQ's limit, we identify NCs with $R = 0.8$ nm as ideal building blocks for IBSCs within this scheme, based on their film's continuous absorption spectrum and high estimated limiting conversion efficiencies.

In the second scheme, the CBM-derived miniband in nanocrystal films is shown to possess all the characteristics of an ideal IB, with the estimated limiting IBSC efficiencies exceeding SQ's limit for a single absorber in films of nanocrystals with $1.2 < R < 3.5$ nm. However in this case, instead of below-band-gap absorption, our scheme enables harnessing of some of the photon energy in excess of the bandgap of the active material, which is usually lost to heating of the cell with consequent degradation of its performance. We identify NC sizes in the range 2 to 3.5 nm as the most suitable for the implementation of this scheme.

We hope that, despite the existence of a number of challenges in the implementation of CQD-based IBSCs, the many advantages highlighted in this study will encourage further exploration and optimization efforts of these systems aimed at the full exploitation of their potential and the fulfilment of their promise to exceed SQ's limit.

SUPPLEMENTARY MATERIAL

Theoretical method, Atomistic modelling of single NCs, 3D Charge densities of isolated NCs, Optical spectra of isolated NCs, 3D band structure of a film of InAs NCs with $R = 0.6$ nm, Absorption edge peak energies in isolated NCs and quantum dot films, 3D oscillator strength in a film of InAs NCs with $R = 1.2$ nm, Evolution of the band structure with dot-to-dot separation in a film of InAs NCs with $R = 1.2$ nm.

ACKNOWLEDGEMENTS

M.C. gratefully acknowledges financial support from the School of Electronic & Electrical Engineering, University of Leeds. F.M.G.C. and S.R.B. were supported by Project ENE2016_80944_R, funded by the Spanish Ministerio de Economía, Industria y Competitividad.

References

(1) Luque, A.; Marti, A. Increasing the Efficiency of Ideal Solar Cells by Photon Induced Transitions at Intermediate Levels *Phys. Rev. Lett.* **1997**, *78*, 5014.

(2) Luque, A.; Marti, A.; Stanley, C. Understanding Intermediate-Band Solar Cells *Nat. Photonics* **2012**, *6*, 146-152.

(3) Marti, A.; Antolin, E.; Linares, P.G.; Luque, A. Understanding Experimental Characterization of Intermediate Band Solar Cells *J. Mater. Chem.* **2012** *22*, 22832-22839.

(4) Linares, P. G.; Marti, A.; Antolin, E.; Farmer, C. D.; Ramiro, I.; Stanley, C. R.; Luque, A. Voltage Recovery in Intermediate Band Solar Cells. *Sol. Energy Mater. Sol. Cells* **2012** *98*, 240-244.

(5) Beattie, N. S.; See, P.; Zoppi, G.; Ushasree, P. M.; Duchamp, M.; Farrer, I.; Ritchie, D. A.; Tomić, S. Quantum Engineering of InAs/GaAs Quantum Dot Based Intermediate Band Solar Cells *ACS Photonics* **2017**, *4*, 2745-2750.

(6) Ekins-Daukes, N.; Honsberg, C.; Yamaguchi, M. Signature of Intermediate Band Materials from Luminescence Measurements, *Conference Record of the Thirty-first IEEE Photovoltaic Specialists Conference*, (IEEE 2005), 49-54. DOI: 10.1109/pvsc.2005.1488066.

(7) Lopez, N.; Reichertz, L. A.; Yu, K. M.; Campman, K.; Walukiewicz, W. Engineering the Electronic Band Structure for Multiband Solar Cells. *Phys. Rev. Lett.* **2010** *106*, 028701.

(8) Vörös, M.; Galli, G.; Zimanyi, G. T. Colloidal Nanoparticles for Intermediate Band Solar Cells. *ACS Nano* **2015**, *9*, 6882-6890.

(9) Landes, C. F., Braun, M., and El-Sayed, M. A. On the Nanoparticle to Molecular Size Transition: Fluorescence Quenching Studies. *J. Phys. Chem. B* **2001**, *105*, 10554-10558.

(10) Gómez-Campos, F. M.; Rodríguez-Bolívar, S.; Califano, M. High-Mobility Toolkit for Quantum Dot Films. *ACS Photonics* **2016**, *3*, 2059-2067.

(11) Jasieniak, J.; Califano, M.; Watkins, S. E. Size-Dependent Valence and Conduction Band-Edge Energies of Semiconductor Nanocrystals *ACS Nano* **2011**, *5*, 5888-5902.

(12) Chestnoy, N.; Harris, T. D.; Hull, R.; Brus, L. E. Luminescence and Photophysics of CdS Semiconductor Clusters: The Nature of the Emitting Electronic State *J. Phys. Chem.* **1986** *90*, 3393-3399.

(13) Kilina, S. V.; Kilin, D. S.; Prezhdo, O. V. Breaking the Phonon Bottleneck in PbSe and CdSe Quantum Dots: Time-Domain Density Functional Theory of Charge Carrier Relaxation *ACS Nano* **2009**, *3*, 93-99.

(14) Jasieniak, J.; Smith, L.; Embden, J. v.; Mulvaney, P.; Califano, M. Re-examination of the Size-Dependent Absorption Properties of CdSe Quantum Dots *J. Phys. Chem. C* **2009**, *113*, 19468-19474.

(15) Gómez-Campos, F. M.; Rodríguez-Bolívar, S.; Skibinsky-Gitlin, E. S.; Califano, M. Efficient, Non-Stochastic, Monte-Carlo-Like-Accurate Method for the Calculation of the Temperature-Dependent Mobility in Nanocrystal Films. *Nanoscale* **2018**, *10*, 9679-9690.

(16) Califano, M.; Gómez-Campos, F. M. Universal Trapping Mechanism in Semiconductor Nanocrystals. *Nano Lett.* **2013**, *13*, 2047-2052.

(17) Zhu, H.; Yang, Y.; Hyeon-Deuk, K.; Califano, M.; Song, N.; Wang, Y.; Zhang, W.; Prezhdo, O. V.; Lian, T. Auger-Assisted Electron Transfer from Photoexcited Semiconductor Quantum Dots. *Nano Lett.* **2014**, *14*, 1263-1269.

(18) Califano, M. Origins of Photoluminescence Decay Kinetics in CdTe Colloidal Quantum Dots *ACS Nano* **2015**, *9*, 2960-2967.

(19) Baker, D. R.; Kamat, P. V. Tuning the Emission of CdSe Quantum Dots by Controlled Trap Enhancement. *Langmuir* **2010**, *26*, 11272-11276.

(20) Chon, J. W. M.;Gu, M.; Bullen, C.; Mulvaney, P. Three-Photon Excited Band Edge

and Trap Emission of CdS Semiconductor Nanocrystals *Appl. Phys. Lett.* **2004** *84*, 4472-4474.

(21) Schaller, R. D.; Pietryga, J. M.; Klimov, V. I. Carrier Multiplication in InAs Nanocrystal Quantum Dots with an Onset Defined by the Energy Conservation Limit *Nano Lett.* **2007**, *7*, 3469-3476.

(22) Krishna, A.; Krich, J. J. Increasing Efficiency in Intermediate Band Solar Cells with Overlapping Absorptions *J. Opt.* **2016**, *18*, 074010-1–074010-7.

(23) Bremner, S. P.; Levy, M. Y.; Honsberg, C. B. Limiting Efficiency of an Intermediate Band Solar Cell under a Terrestrial Spectrum *Appl. Phys. Lett.* **2008**, *92*, 171110.

(24) Shockley, W.; Queisser, H. J. Detailed Balance Limit of Efficiency of p-n Junction Solar Cells *J. Appl. Phys.* **1961**, *32*, 510-519.

(25) Puangmali, T.; Califano, M.; Harrison, P. Monotonic Evolution of the Optical Properties in the Transition from Three- to Quasi-Two-Dimensional Quantum Confinement in InAs Nanorods. *J. Phys. Chem. C* **2010**, *114*, 6901-6908.

(26) Bozyigit, D.; Lin, W. M. M.; Yazdani, N.; Yarema O.; Wood V. A Quantitative Model for Charge Carrier Transport, Trapping and Recombination in Nanocrystal-Based Solar Cells. *Nature Commun.* **2015** *6*, 6180.

(27) Yu, W. W.; Qu, L.; Guo, W.; Peng, X. Experimental Determination of the Extinction Coefficient of CdTe, CdSe, and CdS Nanocrystals. *Chem. Mater.* **2003**, *15*, 2854-2860

(28) Yu, W. W.; Qu, L.; Guo, W.; Peng, X. Experimental Determination of the Extinction Coefficient of CdTe, CdSe and CdS Nanocrystals. *Chem. Mater.* **2004**, *16*, 560

(29) Rajh, T.; Micic, O. I.; Nozik, A. J. Synthesis and Characterization of Surface-Modified Colloidal Cadmium Telluride Quantum Dots. *J. Phys. Chem.* **1993**, *97*, 11999-12003.

(30) Vossmeyer, T.; Katsikas, L.; Giersig, M.; Popovic, I. G.; Diesner, K.; Chemseddine, A.; Eychmuller, A.; Weller, H. CdS Nanoclusters: Synthesis, Characterization, Size Dependent Oscillator Strength, Temperature Shift of the Excitonic Transition Energy, and Reversible Absorbance Shift. *J. Phys. Chem.* **1994**, *98*, 7665-7673.

(31) Yu, P.; Beard, M.; Ellingson, R.; Ferrere, S.; Curtis, C.; Drexler, J.; Luiszer, F.; Nozik, A. Absorption Cross-Section and Related Optical Properties of Colloidal InAs Quantum Dots. *J. Phys. Chem. B* **2005**, *109*, 7084-7087.

(32) Cademartiri, L.; Montanari, E.; Calestani, G.; Migliori, A.; Guagliardi, A.; Ozin, G. A. Size-Dependent Extinction Coefficients of PbS Quantum Dots. *J. Am. Chem. Soc.* **2006**, *128*, 10337-10346.

(33) Moreels, I.; Lambert, K.; Muynck, D.; Vanhaecke, F.; Poelman, D.; Martins, J.; Allan, G.; Henz, Z. Composition and Size-Dependent Extinction Coefficient of Colloidal PbSe Quantum Dots. *Chem. Mater.* **2007**, *19*, 6101-6106.

(34) Xu, Y.; Gong, T.; Munday, J. N. The Generalized Shockley-Queisser Limit for Nanostructured Solar Cells. *Sci. Reports* **2015**, *5*, 13536-1–13536-9.

(35) Strandberg, R.; Reenaas, T. W. Photofilling of Intermediate Bands *J. Appl. Phys.* **2009**, *105*, 124512-1–124512-8.

(36) Ashcroft, N. W.; Mermin, N. *Solid State Physics*, Holt Rinehart and Winston, New York, London, 1976.

(37) Mićić, O. I.; Ahrenkiel, S. P.; Nozik, A. J. Synthesis of Extremely Small InP Quantum Dots and Electronic Coupling in their Disordered Solid Films *Appl. Phys. Lett.* **2001**, *78*, 4022-4024.

(38) Liljeroth, P.; Overgaag, K.; Urbieta, A.; Grandidier, B.; Hickey, S. G.; Vanmaekel-

bergh, D. Variable Orbital Coupling in a Two-Dimensional Quantum-Dot Solid Probed on a Local Scale. *Phys. Rev. Lett.* **2006**, *97*, 096803.

(39) Steiner, D.; Aharoni, A.; Banin, U.; Millo, O. Level Structure of InAs Quantum Dots in Two-Dimensional Assemblies. *Nano Lett.* **2006**, *6*, 2201-2205.

(40) Artemyev, M. V.; Bibik, A. I.; Gurinovich, L. I.; Gaponenko, S.V.; Woggon, U. Evolution from Individual to Collective Electron States in a Dense Quantum Dot Ensemble *Phys. Rev. B* **1999** *60*, 1504-1506.

(41) Choi, J.-H.; Fafarman, A. T.; Oh, S. J.; Ko, D.-K.; Kim, D. K.; Diroll, B. T.; Muramoto, S.; Gillen, J. G.; Murray, C. B.; Kagan, C. R. Bandlike Transport in Strongly Coupled and Doped Quantum Dot Solids: A Route to High-Performance Thin-Film Electronics. *Nano Lett.* **2012**, *12*, 2631-2638.

(42) Lee, J.-S.; Kovalenko, M. V.; Huang, J.; Chung, D. S.; Talapin, D. V. Band-Like Transport, High Electron Mobility and High Photoconductivity in All-Inorganic Nanocrystal Arrays. *Nature Nanotechn.* **2011** *6*, 348-352.

(43) Robel, I.; Kuno, M.; Kamat, P. V. Size-Dependent Electron Injection from Excited CdSe Quantum Dots into TiO2 Nanoparticles. *J. Am. Chem. Soc.* **2007**, *129*, 4136-4137.

(44) Okada, Y. *et al.* Intermediate Band Solar Cells: RecentProgress and Future Directions. *App. Phys. Rev.* **2015**, *2*, 021302-1–021302-48.

(45) Saputra, E.; Ohta, J.; Kakuda, N.; Yamaguchi, K. Self-Formation of In-Plane Ultrahigh-Density InAs Quantum Dots on GaAsSb/GaAs(001). *Appl. Phys. Express* **2012**, *5*, 125502.

(46) Wasilewski, Z. R.; Fafard, S.; McCaffrey, J. P. Size and Shape Engineering of Vertically Stacked Self-Assembled Quantum Dots *J. Cryst. Growth* **1999**, *201-202*, 1131-1135.

(47) Martí, A.; López, N.; Antolín, E.; Cánovas, E.; Luque, A.; Stanley, C. R.; Farmer, C. D.; Díaz, P. Emitter Degradation in Quantum Dot Intermediate Band Solar Cells *Appl. Phys. Lett.* **2007**, *90*, 233510.

(48) Yang, X. ; Wang, . K.; Gu, Y.; Ni, H.; Wang, X.; Yang, T.; Wang, Z. Improved Efficiency of InAs/GaAs Quantum Dots Solar Cells by Si-Doping. *Sol. Energy Mater. Sol Cells* **2013**, *113*, 144-147.

(49) Lantratov, V. M. *et al.* AlGaAs/GaAs Photovoltaic Cells with InGaAs Quantum Dots, *Adv. Sci. Technol.* **2010**, *74*, 231-236.

(50) Liu, W.; Lee, J.-S.; Talapin, D. V. III-V Nanocrystals Capped with Molecular Metal Chalcogenide Ligands: High Electron Mobility and Ambipolar Photoresponse. *J. Am. Chem. Soc.* **2013** *135*, 1349-1357.

(51) Kagan, C. R.; Murray, C. B. Charge Transport in Strongly Coupled Quantum Dot Solids. *Nature Nanotechn.* **2015** *10*, 1013-1026.

(52) Moore, D. T.; Gaskey, B.; Robbins, A.; Hanrath, T. A Detailed Balance Analysis of Conversion Efficiencies Limits for Nanocrystal Solar Cells-Relating the Shape of the Excitonic Peak to Conversion Efficiencies. *J. Appl. Phys.* **2014** *115*, 054313.

(53) Green, M. Multiple Band and Impurity Photovoltaic Solar Cells: General Theory and Comparison to Tandem Cells. *Prog. Photovolt: Res. Appl.* **2001**, *9*, 137-144.